Structure of Fe-Si-melts by X-ray Diffraction

B. Sedelmeyer * and S. Steeb

Max-Planck-Institute for Materials Science, Seestraße 92, D-70174 Stuttgart

Z. Naturforsch. **52a**, 415–419 (1997); received February 26, 1997

X-ray diffraction was done with molten $Fe_{66.7}Si_{33.3}$ and molten $Fe_{33.3}Si_{66.7}$. The coordination numbers versus the concentration lie above the connection line between the coordination numbers of the unalloyed molten elements Fe and Si, respectively, which means a tendency for microsegregation. The pair correlation function of molten $Fe_{66.7}Si_{33.3}$ was modeled using the data of crystalline Fe_2Si. At the same time, the pair correlation function of the molten alloy $Fe_{33.3}Si_{66.7}$ can be modeled using the data of the corresponding crystalline alloy. Thus for molten $Fe_{33.3}Si_{66.7}$ microsegregation into $FeSi_2$ and Si or FeSi and for molten $Fe_{66.7}Si_{33.3}$ microsegregation into Fe_2Si and Fe or FeSi exists.

1. Introduction

In previous papers we showed for Fe-B- [1], Ni-B- [2], Mn-Si- [3], and Ni-P- [4] melts that the second peak of a structure factor and/or of a pair correlation function obtained from a melt shows a splitting up or a shoulder if the corresponding melt yields an amorphous alloy during rapid solidification. The present paper is concerned with a structure investigation of two molten Fe-Si-alloys, namely $Fe_{66.7}Si_{33.3}$ and $Fe_{33.3}Si_{66.7}$. As described in [4] the structure factors $S(Q)$ had to be Fourier-transformed to obtain a $G(R)$-function to which then was given the shape of $G(R) = -4\pi R \varrho_0$ for R-values smaller than the hard sphere diameter. Back transformation into the Q-space yielded the corrected run $S'(Q)$ which oscillates properly around unity.

2. Theoretical Fundamentals

Concerning the fundamentals we refer for example to [4].

3. Experimental

Iron (99.999%) and silicon (99.99%) were alloyed by induction heating and cast as discs with a diameter of 35 mm. The surface of the discs was grinded and the lower side was plain-grinded to yield good thermal contact to the crucible. The diffraction experiments within the θ-θ goniometer were done in 5 mbar He-atmosphere. For $Fe_{66.7}Si_{33.3}$ a ThO_2-crucible and for the $Fe_{33.3}Si_{66.7}$-melt a BN-crucible was used. The ThO_2-crucible was mechanically stabilized by a molybdenum sheet bound tightly along the circumference.

4. Results and Discussion

4.1. Molten $Fe_{66.7}Si_{33.3}$ at 1250 °C

Figure 1, upper curves, show the Faber Ziman structure factor as obtained from the experimental data as solid line and the backtransformed structure factor $S'(Q)$ as broken line. The first peak lies at 3.02 $Å^{-1}$ with a height of 2.92. The second peak lies at 5.32 $Å^{-1}$ (height 1.3) with a shoulder at 5.82 $Å^{-1}$. The third maximum lies at 8.26 $Å^{-1}$ and shows nearly the same width as the second one. All numerical data from the structure factor are compiled in Table 1. Molten $Fe_{70}Si_{30}$ at 50 °C above liquidus was also investigated in [5] and showed the same position of the first peak but with 2.3 a lower height compared to that observed in the present paper. On the other hand, in [6] $Fe_{80}Si_{20}$- and $Fe_{60}Si_{40}$-melts were investigated at 1550 °C, i.e. 200 °C above liquidus. The following data for position, height, and width of the first peak were reported [6] for molten $Fe_{80}Si_{20}$: 3.00 $Å^{-1}$; 2.77 $Å^{-1}$; 0.65 $Å^{-1}$ and for molten $Fe_{60}Si_{40}$: 2.93 $Å^{-1}$; 2.70 $Å^{-1}$; and 0.7 $Å^{-1}$. Higher temperatures yield lower and broader primary peaks. Furthermore, a slight shift to smaller Q-values corresponding to larger distances can be observed with increasing temperature. Thus good accordance is achieved with the present data and those from

* Alcatel SEL, 70430 Stuttgart.

Reprint requests to Prof. Dr. Dr. h.c. S. Steeb.

0932-0784 / 97 / 0500-0415 $ 06.00 © – Verlag der Zeitschrift für Naturforschung, D-72027 Tübingen

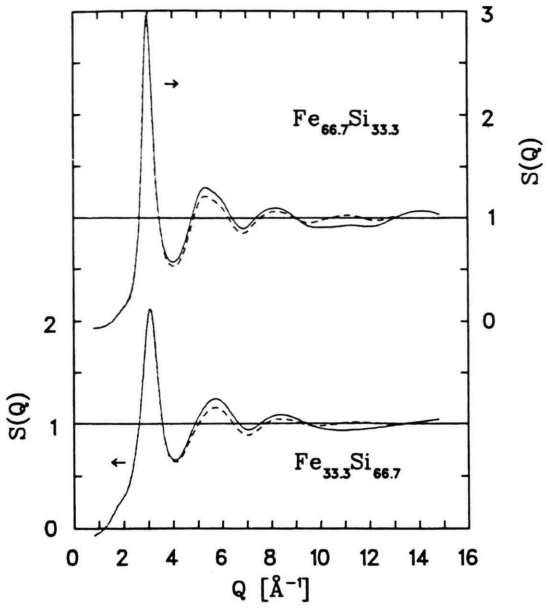

Fig. 1. Faber Ziman structure factors; X-ray diffraction; —— as obtained ($S(Q)$) (Mo-Kα). - - - - corrected ($S'(Q)$). Upper curves: Molten $Fe_{66.7}Si_{33.3}$: 1250 °C. Lower curves: Molten $Fe_{33.3}Si_{66.7}$; 1262 °C.

[5], whereas between [5] and [6] there exist discrepancies.

Figure 2 shows with full line the pair correlation function obtained with molten $Fe_{66.7}Si_{33.3}$. The shortest distance amounts to 2.52 Å with 12.7 nearest neighbours. The second peak lies at 4.55 Å with a small shoulder at 4.96 Å. Table 2 contains all numerical data from the pair correlation functions.

4.1.1. Comparison with amorphous $Fe_{65}Si_{35}$

According to [7], Fe_xSi_{1-x}-alloys can be obtained for all x-values as amorphous films by evaporation onto a cooled substrate. The production of meltspun amorphous Fe-Si-alloys is not possible. By means of electron diffraction [7], amorphous $Fe_{65}Si_{35}$ was investigated up to $Q = 9$ Å^{-1}. The corresponding peak positions are presented in Table 1. The accordance between the structure factor of amorphous $Fe_{65}Si_{35}$ and molten $Fe_{66.7}Si_{33.3}$ is not as good as between amorphous $Ni_{80}P_{20}$ and molten $Ni_{81}P_{19}$ [4], but also for the Fe-Si-alloys a shoulder at the second peak is observed in the amorphous as well as in the molten state.

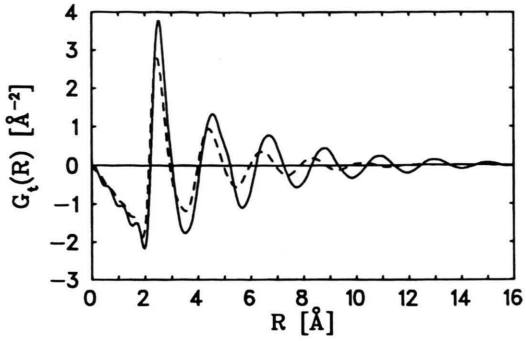

Fig. 2. Faber Ziman pair correlation functions; —— Molten $Fe_{66.7}Si_{33.3}$; 1250 °C. - - - - Molten $Fe_{33.3}Si_{66.7}$; 1262 °C.

Table 1. Structure factors; peak positions, peak heights, widths at half maximum for molten $Fe_{66.7}Si_{33.3}$, molten $Fe_{33.3}Si_{66.7}$, amorphous $Fe_{30}Si_{70}$, and amorphous $Fe_{65}Si_{35}$ [7].

	Molten state		Amorphous state	
	$Fe_{66.7}Si_{33.3}$	$Fe_{33.3}Si_{66.7}$	$Fe_{30}Si_{70}$	$Fe_{65}Si_{35}$
1. Maximum position [Å^{-1}]	3.02	3.15	3.25	3.14
height	2.92	2.10		
width at half maximum [Å^{-1}]	0.51	0.77		
2. Maximum position [Å^{-1}]	5.32	5.72	5.54	5.38
height	1.30	1.16		
width at half maximum [Å^{-1}]	1.50	1.60		
shoulder position [Å^{-1}]	5.82	–	6.02	6.13
1. Maximum position [Å^{-1}]	8.26	8.39		8.05
height	1.07	1.05		
width at half maximum [Å^{-1}]	1.57	1.48		

Table 2. Pair correlation functions; peak positions, half widths and coordination numbers for molten $Fe_{66.7}Si_{33.3}$ and molten $Fe_{33.3}Si_{66.7}$.

	$Fe_{66.7}Si_{33.3}$	$Fe_{33.3}Si_{66.7}$
R_I [Å]	2.52	2.44
ΔR_I [Å]	0.63	0.62
Z_I	12.7	10.1
R_{II} [Å]	4.55	4.37
R_{II} (shoulder) [Å]	4.96	–
ΔR_{II} [Å]	1.13	0.92
Z_{II}	43.7	27.8
R_{III} [Å]	6.69	6.39
ΔR_{III} [Å]	1.04	1.05

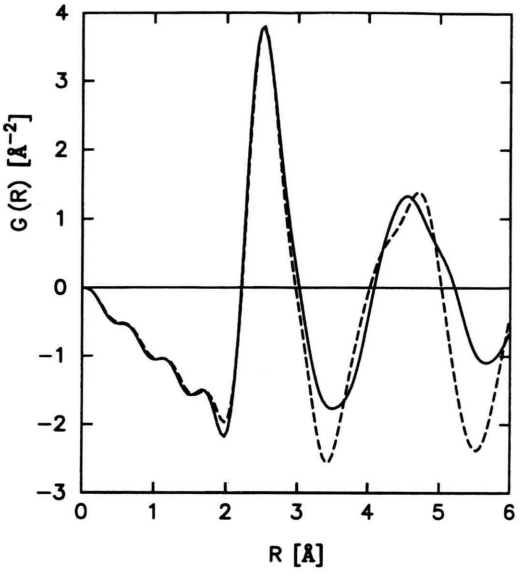

Fig. 3. Faber Ziman pair correlation functions; —— $G_t(R)$ from molten $Fe_{66.7}Si_{33.3}$; 1250 °C. - - - - $G_{mod}(R)$ from crystalline Fe_2Si using half widths σ from Table 3.

Table 3. Coordination numbers Z and atomic distances R for cubic Fe_2Si [8]. The half widths σ are larger than those given in [8], because during modelling the $Fe_{66.7}Si_{33.3}$ with the present σ-values optimum coincidence between experiment and model could be achieved.

Coordination	Z	R [Å]	σ [Å]
Z_{FeSi}	4	2.47	0.41
Z_{FeFe}	2	2.47	0.41
Z_{FeSi}	1	2.86	0.57
Z_{FeFe}	4.5	2.86	0.57
Z_{SiSi}	2.67	2.86	0.57
Z_{FeSi}	2	4.04	0.79
Z_{FeFe}	9	4.04	0.79
Z_{SiSi}	5.33	4.04	0.79
Z_{FeSi}	12	4.73	0.85
Z_{FeFe}	6	4.73	0.85
Z_{FeSi}	1.33	4.96	0.89
Z_{FeFe}	6	4.96	0.89
Z_{SiSi}	3.56	4.96	0.89
Z_{FeSi}	1	5.72	0.99
Z_{FeFe}	4.5	5.72	0.99
Z_{SiSi}	2.67	5.72	0.99
Z_{FeSi}	12	6.23	1.05
Z_{FeFe}	6	6.23	1.05
Z_{FeSi}	4	6.39	1.05
Z_{FeFe}	18	6.39	1.07
Z_{SiSi}	10.67	6.39	1.07
Z_{FeSi}	4	7.00	1.07
Z_{FeFe}	10.67	7.00	1.10
Z_{SiSi}	10	7.00	1.10

4.1.2. Comparison with crystalline Fe_2Si

The comparison between the molten and the crystalline state is of special interest in the case of the $Fe_{66.7}Si_{33.3}$-melt since crystalline Fe_2Si is only stable at high temperatures [8]. The elementary cell shows CsCl-structure with a lattice constant of 2.81 Å. The modelling of the first and second peak of $G(R)$ in Fig. 3 was done according to the method described in [4] using data given in Table 3. In Fig. 3 the position of the first peak shows agreement between the experimental and modelled curve. The second peak shows rather large differences between the experimental and modelled curve. These are caused by a smaller broadening of the higher correlations as given by (9) in [4]. The width of the single correlations is given in Table 3, fourth column.

4.2. Molten $Fe_{33.3}Si_{66.7}$ at 1262 °C

Figure 1, lower curve, shows the total Faber Ziman structure factor of molten $Fe_{33.3}Si_{66.7}$, and Table 1 the corresponding data. The first peak lies at higher Q-values than for $Fe_{66.7}Si_{33.3}$. At low Q-values a so-called prepeak is indicated which points according to [9] to compound formation within the molten state. The second peak shows no shoulder but a slight asymmetry. It lies, as the first and third peak, at higher Q-values than the corresponding peaks of $Fe_{66.7}Si_{33.3}$. In [10] a melt with the same alloy composition was investigated using Mo-Kα radiation at a temperature which was 22 °C lower than in the present case. In [10] the first peak was observed at the higher Q-value of 3.3 $Å^{-1}$. The peak position of the first peak of the pair correlation function, however, is with 2.45 Å [10] the same as in the present paper (2.44 Å). The same stands for the coordination number: 9.7 in [10] compared to 10.1 in the present paper.

Figure 2 shows the pair correlation function for molten $Fe_{33.3}Si_{66.7}$ as broken line. The distances are throughout smaller than for molten $Fe_{66.7}Si_{33.3}$, and no shoulder at the second peak is visible.

4.2.1. Comparison with amorphous $Fe_{30}Si_{70}$

Table 1 contains the data from the structure factors of the $Fe_{66.7}Si_{33.3}$- and the $Fe_{33.3}Si_{66.7}$-melt besides those of amorphous $Fe_{65}Si_{35}$ [7] and amorphous $Fe_{30}Si_{70}$ [7]. The position of the first peak of the $Fe_{33.3}Si_{66.7}$-melt lies at smaller Q (3.15 $Å^{-1}$) than that of amorphous $Fe_{30}Si_{70}$ (3.25 $Å^{-1}$).

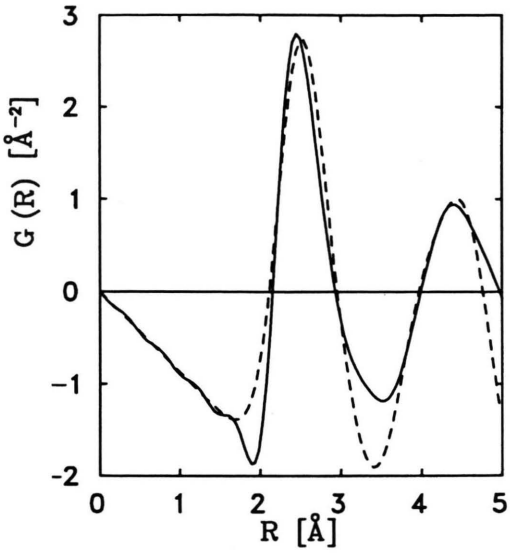

Fig. 4. Faber Ziman pair correlation functions; —— $G_t(R)$ from molten $Fe_{33.3}Si_{66.7}$. - - - - $G_{mod}(R)$ from crystalline $FeSi_2$.

Table 4. Coordination numbers Z and atomic distances R as determined from tetragonal $FeSi_2$ [13] for the calculation of $G_{mod}(R)$. The σ-values led to an optimum coincidence between experiment and model.

Coordination	Z	R [Å]	σ [Å]
Z_{FeSi}	8	2.47	0.65
Z_{SiSi}	1	2.47	0.65
Z_{FeFe}	4	2.82	0.90
Z_{SiSi}	4	2.82	0.90
Z_{SiSi}	1	2.91	0.57
Z_{SiSi}	4	3.75	0.65
Z_{FeFe}	4	3.99	0.67
Z_{SiSi}	4	3.99	0.67
Z_{SiSi}	4	4.05	0.67
Z_{FeSi}	8	4.41	0.70
Z_{FeSi}	16	4.68	0.80
Z_{SiSi}	2	5.39	0.90
Z_{FeFe}	2	5.39	0.97
Z_{SiSi}	4	5.64	0.97
Z_{FeFe}	4	5.64	0.97
Z_{FeSi}	16	5.94	0.97
Z_{SiSi}	8	6.08	1.00
Z_{FeFe}	8	6.08	1.00
Z_{SiSi}	4	6.15	1.03
Z_{FeFe}	8	6.30	1.07
Z_{SiSi}	8	6.30	1.07
Z_{SiSi}	4	6.39	1.07

For the Fe_x-Si_{1-x}-melts the second peaks of the structure factor and of the pair correlation function show only weak shoulders for $x = 66.7$ and only slight asymmetries for $x = 33.3$. Thus these effects are smaller than for molten $Ni_{81}P_{19}$ [4] or molten $Fe_{80}B_{20}$ [1]. If we regard the fact that amorphous Fe_x-Si_{1-x} specimens can only be produced by evaporation as thin films, whereas $Ni_{81}P_{19}$ [11] and $Fe_{80}B_{20}$ [12] can be produced by melt-spinning as thick amorphous ribbons, the conclusion may be allowed that a shoulder or an asymmetry in the second peak of the structure factor or the pair correlation function depend on the difficulties which may arise during the production of amorphous specimens from the melt.

4.2.2. Comparison with crystalline $FeSi_2$

Table 4 contains the distances and coordination numbers as obtained from tetragonal $FeSi_2$ ($a = 2.684$ Å, $c = 5.128$ Å) together with the σ-values as used to calculate $G_{mod}(R)$. This function is given as broken line in Fig. 4 together with $G_{tot}(R)$ for molten $Fe_{33.3}Si_{66.7}$. The first peaks of $G_{tot}(R)$ and $G_{mod}(R)$ coincide concerning the peak height and the position of the middle of the peak width at half maximum. The peak position of $G_{mod}(R)$, however, is shifted to a larger Q value. The coordination number amounts to 10.1 for the melt and to 10.6 for the model. The position of the second peak is the same in both cases but the width of the broken line is smaller. The coordination number amounts to 26.8 atoms in the model compared to 27.8 atoms in the melt. Thus the agreement in the first two peaks for the melt and the corresponding crystalline state is rather good. This agreement means that in the region of the nearest neighbours the chemical interaction between the atoms is nearly the same, independent of whether one regards the molten or the corresponding crystalline state.

5. Type of the Fe-Si-melts

Figure 5 shows the coordination numbers for molten $Fe_{33.3}Si_{66.7}$ and $Fe_{66.7}Si_{33.3}$ versus the Fe-concentration together with the coordination number for unalloyed Fe. The coordination number for solid Si amounts to 4. The coordination number for molten Si is not known. If we assume this coordination number to be between 4 and 8, all the straight connection lines between Z_{Si} and Z_{Fe} lie within the hatched region, and anyhow below the coordination numbers of the Fe-Si-melts. According to [9] this means segregation tendency. Together with the similarity of the $G(R)$-

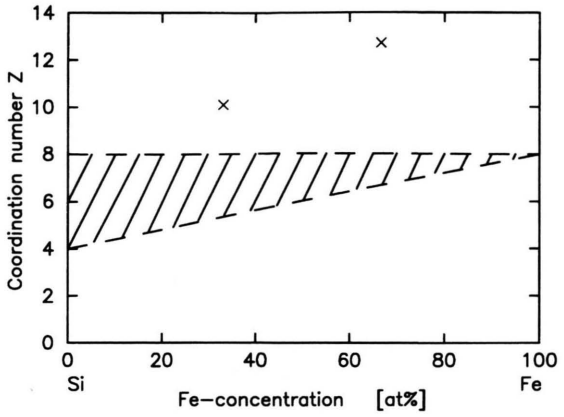

Fig. 5. Fe-Si melts; Coordination numbers versus concentration.

curves of the Fe-Si-melts with their corresponding crystalline structures, this means for molten $Fe_{33.3}Si_{66.7}$ microsegregation into $FeSi_2$ and Si or FeSi, and for molten $Fe_{66.7}Si_{33.3}$ microsegregation into Fe_2Si and Fe or FeSi.

6. Summary

X-ray diffraction was done, using a θ-θ diffractometer, with the two melts $Fe_{66.7}Si_{33.3}$- and $Fe_{33.3}Si_{66.7}$. One finds a slight shoulder at the second peak of the structure factor and the pair correlation function of the $Fe_{66.7}Si_{33.3}$-melt, whereas with the $Fe_{33.3}Si_{66.7}$-melt only an asymmetry can be observed. The coincidence in the total pair correlation functions of amorphous $Fe_{65}Si_{35}$ and molten $Fe_{66.7}Si_{33.3}$ is not so good as in the case of Ni-P-alloys, whereas a good accordance is observed in the first two peaks of $G(R)$, if obtained from the melt or modeled using the data of crystalline Fe_2Si.

The structure factor of molten $Fe_{33.3}Si_{66.7}$ shows an indication of a prepeak which means compound formation within this melt. In the two first peaks of the total pair correlation function of the melt compared to that modeled using the data of crystalline $FeSi_2$ there is good agreement.

The concentration dependence of the coordination numbers shows that in both melts microsegregation occurs.

[1] E. Nold, G. Rainer-Harbach, P. Lamparter, and S. Steeb, Z. Naturforsch. **38a,** 325 (1983).
[2] E. Nassif, P. Lamparter, B. Sedelmeyer, and S. Steeb, Z. Naturforsch. **38a,** 1098 (1983).
[3] E. Nassif, P. Lamparter, B. Sedelmeyer, and S. Steeb, Z. Naturforsch. **38a,** 1093 (1983).
[4] B. Sedelmeyer and S. Steeb, Z. Naturforsch. **52a,** 284 (1997).
[5] Z. Morita, S. Kita, and M. Zeze, Proc. 8th Japan-USSR Joint Symposium on Physical Chemistry of Metallurgical Processes, 24–35 (1981).
[6] Y. Waseda and K. Jakob, Arch. Eisenhüttenwesen **52,** 131 (1981).
[7] Ph. Mangin, G. Marchal, B. Rodmacq, and C. Janot, Phil. Mag. **36,** 643 (1977).
[8] K. Khalaff and K. Schubert, J. Less-Comm. Met. **35,** 341 (1974).
[9] S. Steeb and H. Entress, Z. Metallkde. **57,** 803 (1966).
[10] N. A. Vatolin and E. A. Pastuhov, 4th Japan-USSR Joint Symposium on Phys. Chem. of Metallurgical Processes, 1–12 (1973).
[11] W. Sperl, Doctor Thesis, University of Stuttgart (1982).
[12] E. Nold, Doctor Thesis, University of Stuttgart (1981).
[13] K. Schubert, Kristallstrukturen zweikomponentiger Phasen, Springer-Verlag, Berlin 1964.